OPTIMIZING TIME-DOMAIN NETWORK ANALYSIS

Donald C. DeGroot and Roger B. Marks
National Institute of Standards and Technology, Microwave Metrology Group
Mail Code 813.06, 325 Broadway, Boulder, CO 80303-3328
(303) 497-7212 degroot@boulder.nist.gov

Abstract—In this work, we demonstrate how changes in sample density, time-window size, and waveform averaging affect the accuracy and acquisition time of calibrated time-domain network analysis. One of the key results from this study is that accuracy can be enhanced by eliminating the incident step-edge signal from the time-domain reflection waveform before maximizing the instrument's vertical scale. This study identifies the trade-offs between accuracy and measurement speed and examines other trends to provide general guidance in establishing reliable and efficient time-domain network analysis measurements for a variety of rf and microwave applications.

I. INTRODUCTION

Time-domain network analysis (TDNA), the acquisition of frequency-domain network parameters using time-domain reflection/transmission (TDR/T) instrumentation, is emerging as a cost-effective alternative to traditional frequency-domain network analysis (FDNA). Due to the lower costs of TDR/T instruments, TDNA may find significant application in competitive industries like wireless communications, where amortizing the cost of expensive test equipment can significantly increase component price. Though the concept was proposed nearly three decades ago [1], recent advances in instrumentation [2] and improved calibration techniques [3,4] have made the application of TDNA to rf and microwave measurements practical today. Until recently [3-5], there have been few demonstrations of fully calibrated TDNA device measurements. Consequently, there has been little guidance in establishing appropriate parameters and instrument settings for automated TDNA systems. Though several authors [3-8] have addressed calibration issues and others [9,10] have shown how certain TDR/T instrument settings affect the signal-to-noise ratio of the raw Fourier-transformed waveforms, none of these has illustrated the effects of various instrument parameters on the desired results—calibrated device data.

In this paper, we demonstrate how sample density, time-window length, waveform averaging, and other TDR/T settings affect calibrated TDNA accuracy. To accomplish this, we compared TDNA data collected from coplanar waveguide (CPW) devices for various instrument states to accurate FDNA measurements of the same devices. Since increasing sample density, acquired waveform length, and the number of waveform averages increases acquisition time, this study identifies the trade-offs between accuracy and measurement speed. One particular innovation we discuss offers significantly increased accuracy while slightly reducing acquisition time. Specifically, we show that the incident step-edge signal can be eliminated from the acquired waveform when using an internally stabilized source. While in principle this method should not affect the calibrated results, it greatly increases accuracy by allowing expansion of the instrument's vertical scale. These findings provide guidance in selecting instrument settings for the acquisition of accurate TDNA data, and they may prove useful in future instrumentation developments.

II. MEASUREMENT SYSTEM

We used the time-domain network analyzer system illustrated in Fig. 1 to collect data from CPW calibration structures and test devices on a single GaAs wafer [11]. The system consists of a microwave probe station, a digital sampling oscilloscope (DSO) with TDR/T sample/source heads, and a desk-top computer for automated data acquisition and calibration. The TDR/T heads are mounted on the positioners directly behind the wafer probes. Semi-rigid coaxial cables, 16 mm long with 3.5 mm connectors electrically connect the heads to the probes, and extender cables connect the heads to the DSO. A GPIB connection provides the data and control path between the computer and oscilloscope. The computer runs two independent programs, both developed at NIST. The first controls the DSO, acquires TDR/T waveforms, and performs a fast Fourier transform (FFT) of the data. The second, MultiCal, calibrates the data by removing the systematic imperfections of instrument and connections using the multiline TRL (through-reflect-line) method [12].

For typical measurements, we selected instrument settings and configured the oscilloscope with our acquisition software. The wafer was loaded onto the probe station chuck and the probes were lowered onto the device under test (DUT). The acquisition software collected data in the forward direction: it turned on the fast rise-time step-edge source in the Port 1 TDR/T head, sampled the reflection signal at Port 1, and sampled the transmission signal with the Port 2 TDR/T head. The software then collected data in the reverse direction in a corresponding manner. These time-domain waveforms were transformed into the frequency-domain using the Nicolson FFT method [13], with the results stored to disk for subsequent processing. Figure 2 shows the magnitude of the raw FFT output for waveforms collected using 256 averages. The top trace is from a step-edge signal transmitted through a 20 mm long CPW line. Though the spectrum rolls off strongly with frequency, as expected for a step function, the effective signal strength at 20 GHz is still significantly above the noise floor measured with a 56 Ω resistor terminating the wafer probe.

After data were acquired for all the multiline TRL structures and selected test devices, they were calibrated using the MultiCal software as previously described [4]. MultiCal computed corrected network parameters for selected devices. Figures 3 and 4 show typical TDNA results from this process, along with calibrated FDNA measurements of the same devices. Figure 3 shows the S_{21} magnitude and phase for the 20 mm long CPW line (delay time ≈ 0.18 ns), and Fig. 4 shows the real part of the impedance for a CPW resistor. For both devices, there is good agreement between TDNA and FDNA parameters over a broad frequency band.

One of the key assumptions in our TDNA method is source repeatability. During measurements of all TRL standards and devices, the source must faithfully reproduce the same voltage at the same time relative to the timebase trigger. In practice, this is difficult. A previous report [4] from this laboratory used an external procedure to correct time drift in the source, and another [10] described an internal instrument correction algorithm. In this work, we enabled the internal drift correction of the DSO. We discovered that the degree of drift correction depended on the number of waveform averages selected. For example, the step edge drifted 3 ps in a 30 minute period when the number of averages was set to 32. The frequency-domain phase error ($\Delta\phi$) in degrees is simply related to the time offset (Δt) by

$$\Delta\phi = f \bullet \Delta t \bullet 360, \tag{1}$$

where f is the frequency. A 3 ps drift generates a phase error greater than 10° at 10 GHz. However, we found that the timebase stabilized dramatically when the internal algorithm was applied with increased averaging. The measured drift reduced to less than 0.5 ps for 256 averages. Calibration procedures were not performed with less than 256 averages in this study.

III. RESULTS AND DISCUSSION

Proposed formulas [9,10] for the signal-to-noise ratio (SNR) in TDNA show a direct relation to the sample density and number of averages and an inverse relation to the time-window duration. Three experiments were conducted to investigate these effects in calibrated TDNA, along with one to study waveform truncation. Each are described and discussed separately.

A. Incident Edge Removal

The first experiment examined the elimination of the incident edge from the acquired time-domain reflection signal. Figure 5 shows time-domain reflection records from measurements of the 56 Ω resistor when the incident edge is included and when it is eliminated. In the first case, the sampler acquires the incident edge from the source. Approximately 2 ns later (the round trip time from source to device and back), the sampler records the reflection at the resistor. For loads approximately matched to the system's characteristic impedance, this reflection is small compared to the source signal. Since the vertical scale of the DSO is quantized by the number of bits in the analog-to-digital converter, many of the features of the small reflections are lost. If the timebase is adjusted to start recording data from a repeatable point after the incident edge but before any reflections from the test devices (1 ns past the incident, in this case), the vertical scale can be expanded to recover detail in the signal. The dotted trace in Fig. 5 shows this.

Figure 6 shows the dramatic improvement this method can have in the calibrated TDNA data. For loads with large reflection coefficients, the improvement is not as great; for a short circuit the advantage is almost negligible, while for an open circuit, the vertical resolution can be doubled. All other data presented in this paper, including Figs. 3 and 4, were collected without recording the incident edge.

It is important to understand why the calibration does not require data from the incident edge. In FDNA, a reference signal (*a*) is measured along with the transmitted or reflected signal (*b*) to obtain normalized network parameters (*b/a*). In the present TDNA method, the source is not measured but is assumed to be the same for all loads, both in magnitude and timing. The frequency-domain data from the FFT are not the ratio of unknown to reference; rather, they are the raw signal strength as a function of frequency of the transformed TDR/T waveforms. As long as the incident edge always occurs at the same time relative to the trigger, truncating the TDR wave to eliminate the incident edge is equivalent to subtracting a fixed function of frequency from each reflection spectrum. As long as the calibration method represents the correction as an error matrix, subtracting a fixed function of frequency merely modifies the error matrix. Removal of the incident signal should work with any of the standard calibration methods, not just the multiline TRL used here.

B. Increasing Sample Density

In the next test, we examined how TDNA performance changed as we increased the number of sample points while maintaining a fixed 10.24 ns time window (waveform duration) and 256 waveform averages. Figures 7 and 8 depict the difference between the TDNA and FDNA data from the 20 mm line and CPW resistor for three separate calibrations of differing numbers of samples per ns. Since the number of points in the TDNA frequency-domain records did not match the number of points in the FDNA record, the FDNA data were linearly interpolated before taking the differences. For further comparison, rms values of the $|S_{21}|$ and $|Z|$ difference curves were calculated for 0-10 GHz and 0-20 GHz ranges using

$$\Delta_{rms} = \sqrt{\frac{\sum_{i} D_i^2}{N}} \,,$$ (2)

where D_i is the difference value at point i, and N is the total number of points in the range. Table I lists these figures of merit along with the time required to acquire two-port data from one device.

TABLE I
CHANGES IN SAMPLE DENSITY

Sample Density (ns⁻¹)	$\Delta|S_{21}|$ rms 0-10 GHz (dB)	$\Delta|S_{21}|$ rms 0-20 GHz (dB)	$\Delta|Z|$ rms 0-10 GHz (Ω)	$\Delta|Z|$ rms 0-20 GHz (Ω)	Measurement Time (min:sec)
50	0.0711	0.470	0.421	1.01	0:55
100	0.0529	0.195	0.384	0.717	1:12
200	0.0780	0.303	0.318	0.534	1:45

In Fig. 7 and the corresponding table columns, there is a clear improvement when increasing from 50 ns⁻¹ to 100 ns⁻¹. The sample density of 50 ns⁻¹ corresponds to an effective sampling rate of 50 GS/s and a Nyquist frequency of 25 GHz. Since this may be too low to obtain good data to 20 GHz, there is a significant improvement when increasing to 100 ns⁻¹. Further improvements in S_{21} data for 200 ns⁻¹ are not observed. The limit of repeatability or drift correction may have been achieved for the transmission measurements at 100 ns⁻¹. For the reflection measurements, however, the accuracy of the TDNA Z data consistently improves for increasing sample density.

C. Increasing Time Window Length

Using a 100 ns⁻¹ sample density and 256 averages, we then performed calibrated TDNA measurements for three time-window lengths: 5.12 ns, 10.24 ns and 20.48 ns. In order to maintain 100 ns⁻¹, the total number of points changed for each window length. Figures 9 and 10 and Table II show the results from this experiment.

TABLE II
CHANGES IN TIME WINDOW LENGTH

Window Length (ns)	$\Delta|S_{21}|$ rms 0-10 GHz (dB)	$\Delta|S_{21}|$ rms 0-20 GHz (dB)	$\Delta|Z|$ rms 0-10 GHz (Ω)	$\Delta|Z|$ rms 0-20 GHz (Ω)	Measurement Time (min:sec)
5.12	0.0815	0.316	0.397	0.858	0:55
10.24	0.0529	0.195	0.384	0.717	1:12
20.48	0.0645	0.184	0.444	0.871	1:45

The 0-10 GHz S_{21} data and the Z data improve as the window length increases from 5.12 ns to 10.24 ns. However, the Z data for a window length of 20.48 ns are worse than for the 5.12 ns or 10.24 ns windows. It appears that the window length must be based on the response time of the DUT. In Fig. 5, the response of the resistor has not settled by 5 ns. By 10 ns, the response is stable. Windows shorter than the response time introduce error and windows much longer than the response time may add noise as predicted by [10]. Since the calibration methods require the frequency span and number of points to exactly match for all the standards and devices under test, different window lengths cannot be chosen for specific devices. One time window must be chosen for a given measurement sequence.

D. Increasing Number of Averages

To examine the effects of increasing the number of averages, a single calibration was performed with a 100 ns^{-1} sample density, a 20.48 ns window length, and 1024 averages. The 20 mm line and CPW resistor were measured with differing numbers of waveform averages and then calibrated using the data collected with 1024 averages. Figures 11 and 12 along with Table III show the results.

TABLE III
CHANGES IN THE NUMBER OF WAVEFORM AVERAGES

Num. Averages	$\Delta|S_{21}|_{rms}$ 0-10 GHz (dB)	$\Delta|S_{21}|_{rms}$ 0-20 GHz (dB)	$\Delta|Z|_{rms}$ 0-10 GHz (Ω)	$\Delta|Z|_{rms}$ 0-20 GHz (Ω)	Measurement Time (min:sec)
2	0.338	1.03	2.89	9.12	0:17
4	0.245	0.715	1.66	5.29	0:20
16	0.141	0.404	0.885	2.78	0:23
64	0.0692	0.226	0.568	1.39	0:40
256	0.0569	0.203	0.363	0.777	1:45
1024	0.0484	0.168	0.327	0.599	6:07

The TDNA accuracy consistently improves for increasing number of averages, though this comes at the expense of increasing measurement time. As the number of averages exceeds 64, the rate of decrease in the rms values starts to diminish. In other words, there seems to be less accuracy enhancement and much more time penalty when increasing the number of averages from 256 to 1024 than from 16 to 64. As mentioned above, the time stability of our TDR/T equipment depended on the averaging. Part of the improvement at a low number of averages may be due to an increase in time stability. The smaller changes at high numbers of averages may indicate the TDNA accuracy is approaching an intrinsic instrumentation limit.

IV. CONCLUSIONS

The calibrated TDNA measurements presented in this work show good agreement with FDNA data for the devices measured. The paper demonstrates the practical measurement accuracy expected for a number of instrumentation settings. The results did not show monotonic improvements in data quality with increasing sample density and decreasing time-window length as might have been expected [9,10]. TDNA accuracy improved consistently with increasing waveform averaging, but the returns were marginal at high numbers of averages where the measurement times became long. Since this study looked at a broadband application, the range of sample densities was limited to those above 50 ns^{-1}. Smaller-bandwidth applications may see larger effects for increasing sample densities, but we did not see a significant improvement when increasing from 5 times the Nyquist criterion to 10 times. Changing the time window revealed the importance of selecting a duration longer than the response time of the slowest device to be measured. Increases beyond this appear to diminish TDNA data quality.

The most dramatic improvement to TDNA came from the truncation of the TDR/T signals to eliminate the incident edge from the acquired reflection waveform. This edge removal allows an increase in vertical resolution for TDR data, which improves the determination of small reflection coefficient devices. Application of internal drift correction makes this possible, because the edge is not needed as a fiducial for external processing. Dithering, the application of a noise source to the TDR/T signal, can also overcome the quantization effects of digital TDR/T instruments, but this comes at the cost of increased averaging. Removing the incident edge improves accuracy while actually decreasing data acquisition times.

Although this study used on-wafer measurements to demonstrate the effects of instrument settings, the techniques are generally applicable to other TDNA implementations. These trends should hold for fixtured device and packaging measurements as well, providing guidance in the establishment of automated TDNA systems.

ACKNOWLEDGMENTS

REFERENCES

[1] A. M. Nicolson, "Broad-band microwave transmission characteristics from a single measurement of the transient response," *IEEE Trans. Instrum. Meas.*, vol. 17, no. 4, pp. 395-402, December 1968.

[2] D. A. Smolyansky, S. K. Diamond, and V. K. Tripathi, "Accurate determination of the impedance profile using enhanced accuracy time domain reflection and transmission measurements," 44th ARFTG Conference, Boulder, CO, 1994.

[3] P. Ferrari, G. Angénieux, and B. Fléchet, "A complete calibration procedure for the time domain network analyzers," IEEE MTT-S International Microwave Symposium, Albuquerque, NM, 1992.

[4] R. B. Marks, L. A. Hayden, J. A. Jargon, and F. Williams, "Time domain network analysis using the multiline TRL calibration," 44th ARFTG Conference, Boulder, CO, 1994.

[5] R. B. Marks, D. C. DeGroot, and J. A. Jargon, "High-speed interconnection characterization using time domain network analysis," *Advancing Microelectronics*, vol. 22, November-December. 1995.

[6] W. R. Scott Jr., and G. S. Smith, "Error corrections for an automated time-domain network analyzer," *IEEE Trans. Instrum. Meas.*, vol. 35, no. 3, pp. 300-303, September, 1986.

[7] L. A. Hayden, and V. K. Tripathi, "Calibration methods for time domain network analysis," *IEEE Trans. Microwave Theory Tech.*, vol. 41, no. 3, pp. 415-420, March, 1993.

[8] W. Su, and S. M. Riad, "Calibration of time domain network analyzers," *IEEE Trans. Instrum. Meas.*, vol. 42, no. 2, pp. 157-161, April, 1993.

[9] S. Diamond, and S. Pepper, "Decode dynamic range in time/frequency domain analyzers," *Microwaves and RF*, pp. 102-110, September, 1993.

[10] L. A. Hayden, R. B. Marks, and J. B Rettig, "Accuracy and repeatability in time domain network analysis," 44th ARFTG Conference, Boulder, CO, 1994.

[11] D. Williams, R. Marks, K. Phillips, and T. Miers, "Progress toward MMIC on-wafer standards," 36th ARFTG, 1994.

[12] R. B. Marks, "A multiline method of network analyzer calibration," *IEEE Trans. Microwave Theory Tech.*, vol. 39, no. 7, pp. 1205-1215, July, 1991.

[13] A. M. Nicolson, "Forming the fast Fourier transform of a step response in time-domain metrology," *Electron. Lett.*, vol. 9, no. 14, pp 317-318, 12 July, 1973.
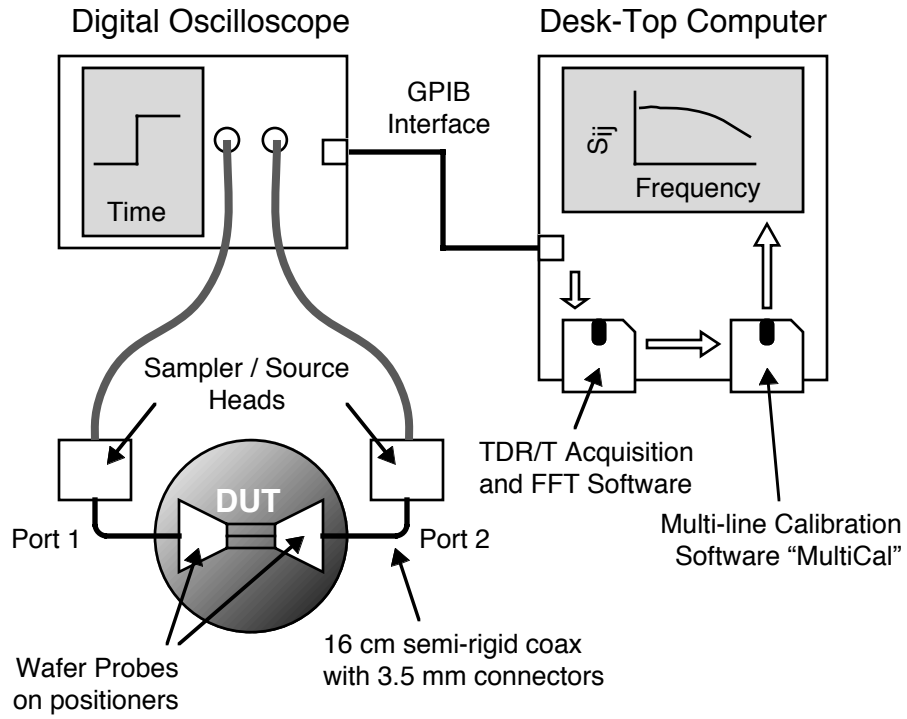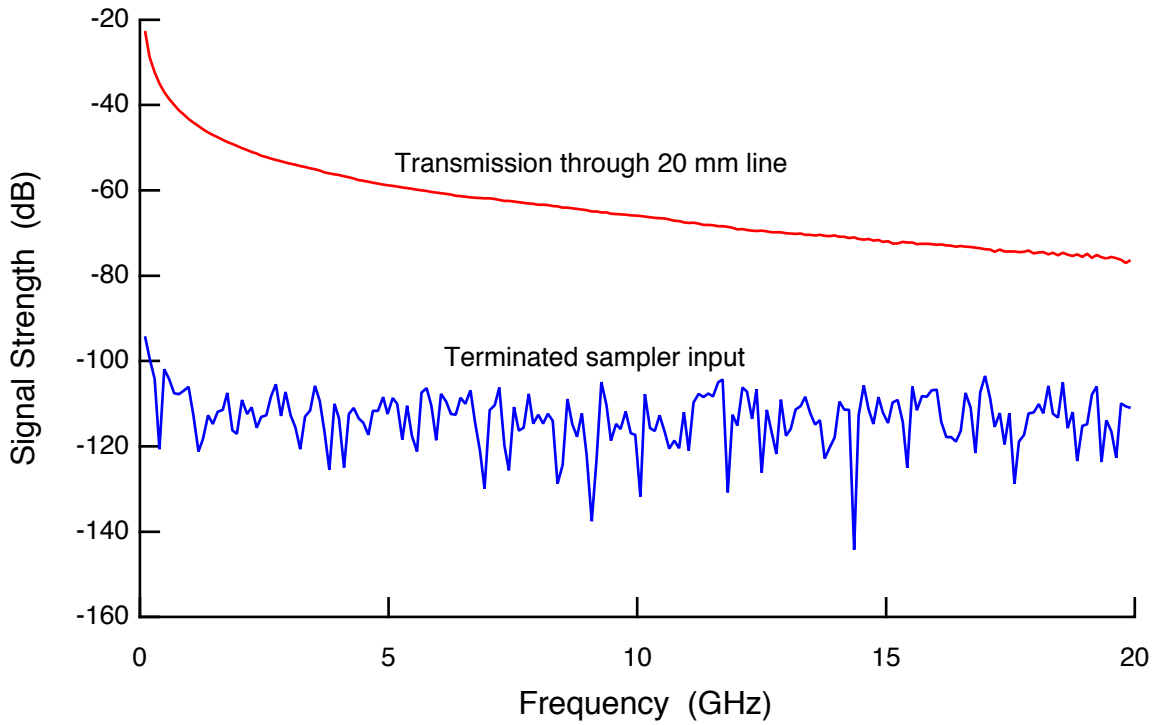
Fig. 1. TDNA Measurement System.
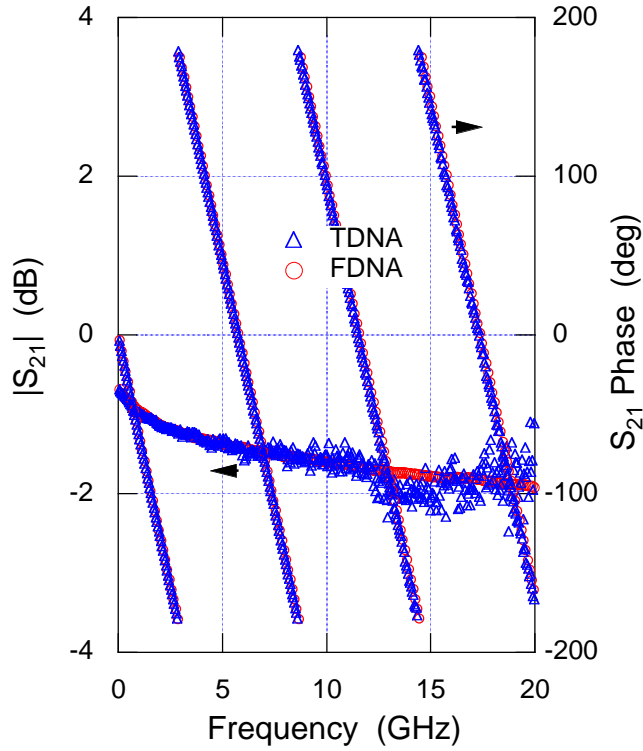

Fig. 2. Raw FFT output of TDR/T waveforms.

Fig. 3. S$_{21}$ data for 20 mm CPW line from FDNA and TDNA.
TDNA Settings: 100 ns^{-1}, 20.48 ns Window, 1024 averages.
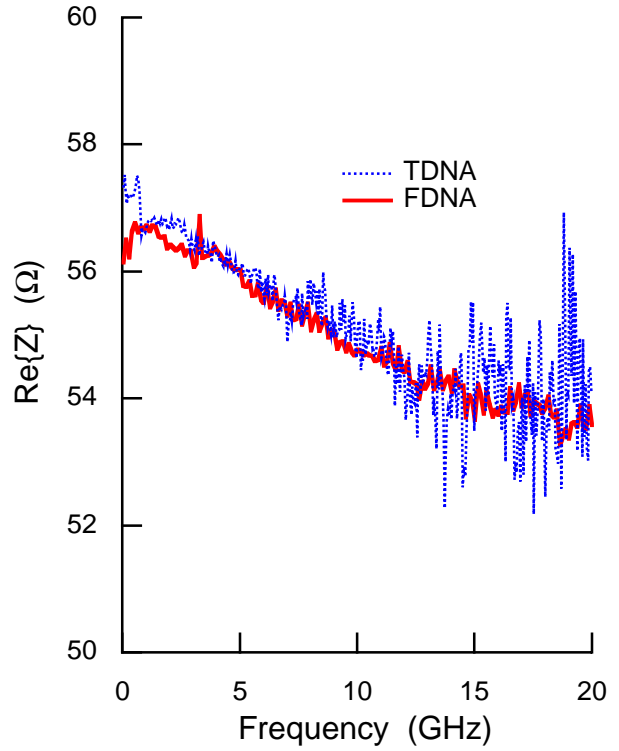

Fig. 4. Impedance data for resistor from FDNA and TDNA.
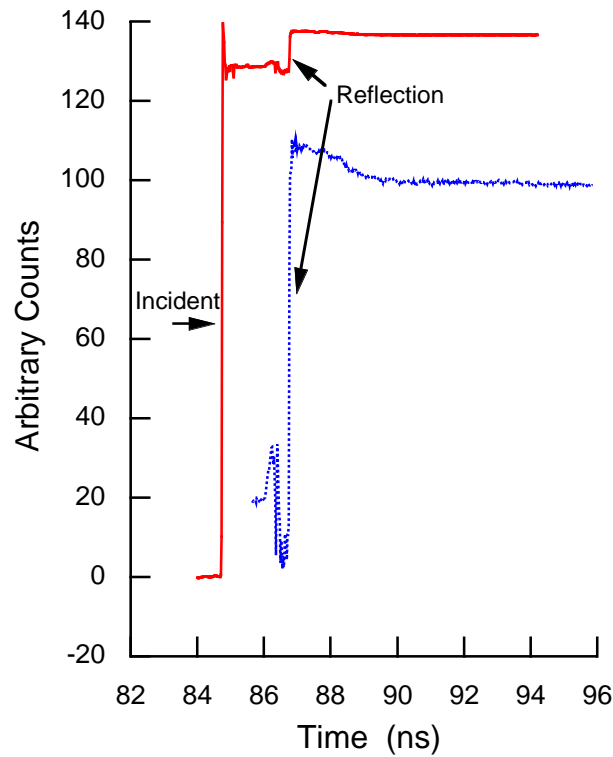TDNA Settings: 100 ns^{-1}, 20.48 ns Window, 1024 averages.

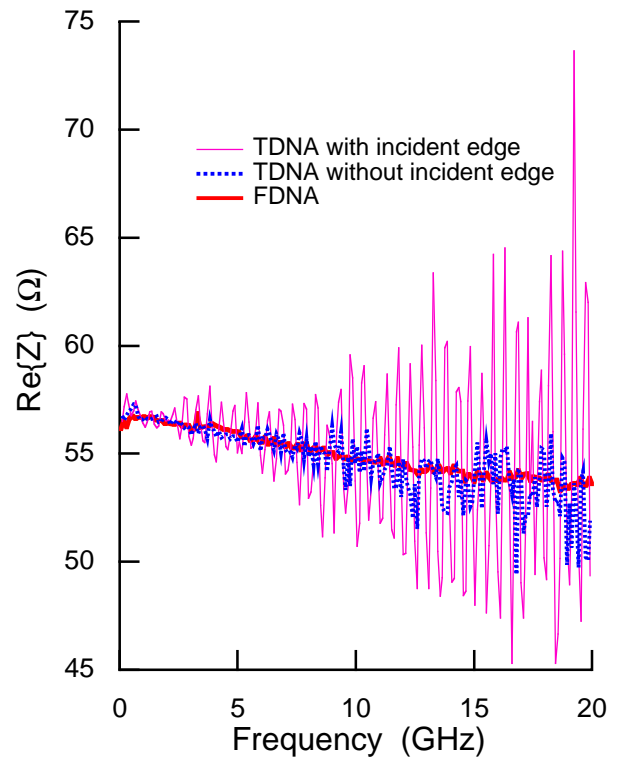Fig. 5. TDR waveforms from CPW resistor, with and without
incident edge.

Fig. 6. Comparison of TDNA data collected with and without
incident edge for CPW resistor.
TDNA Settings: 50 ns^{-1}, 5.12 ns Window, 256 avgs.
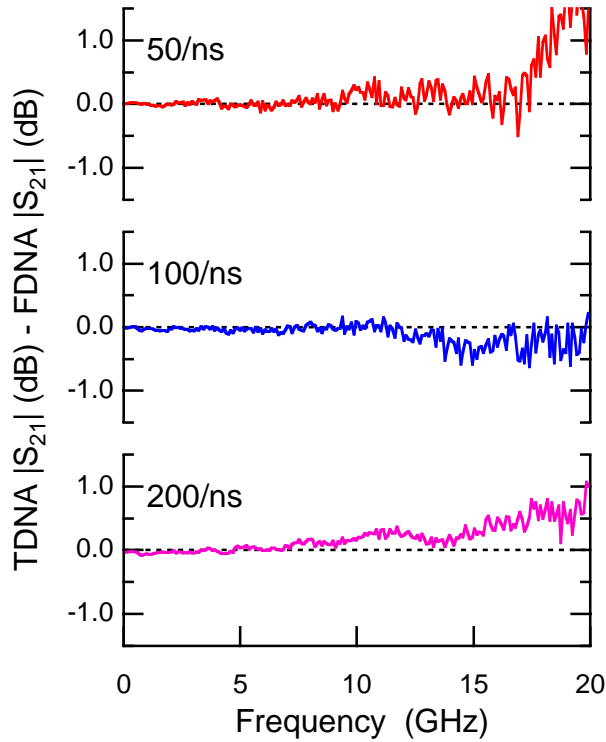
Fig. 7. Difference between TDNA and FDNA in S_{21} data from 20 mm line with differing sample densities.
TDNA Settings: 10.24 ns Window, 256 avgs.
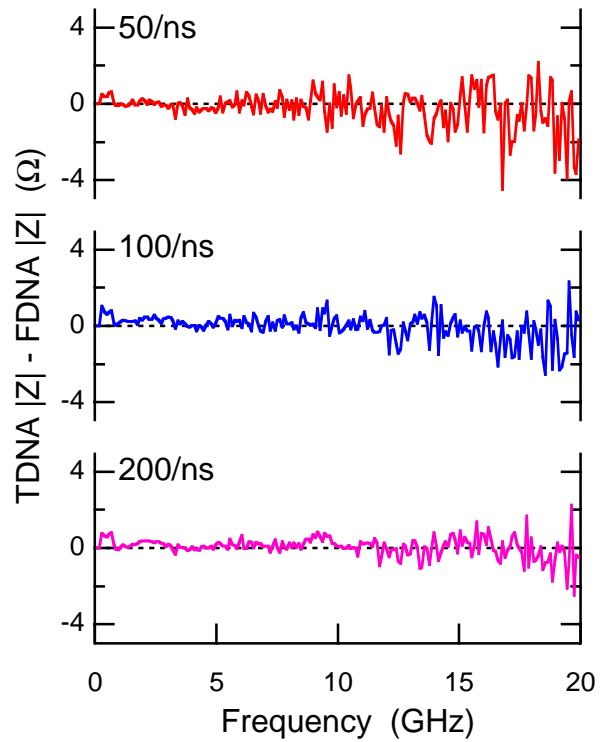
Fig. 8. Difference between TDNA and FDNA in Z data from CPW resistor with differing sample densities.
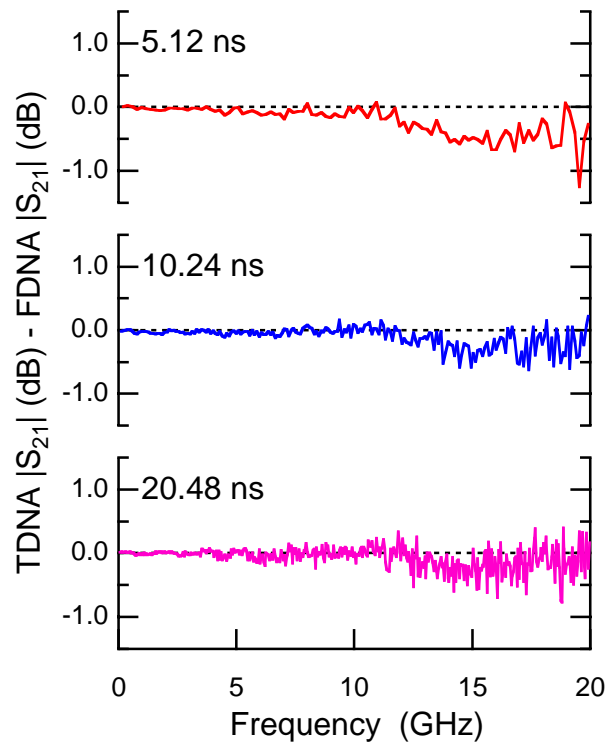TDNA Settings: 10.24 ns Window, 256 avgs.

Fig. 9. Difference between TDNA and FDNA in S_{21} data from 20 mm line with differing window lengths.
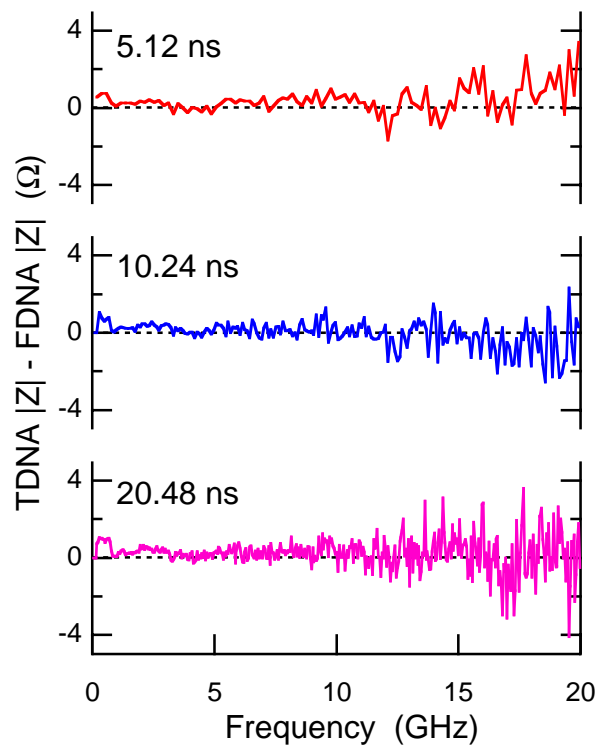TDNA Settings: 100 ns^{-1}, 256 avgs.

Fig. 10. Difference betweem TDNA and FDNA in Z data from CPW resistor with differing window lengths.
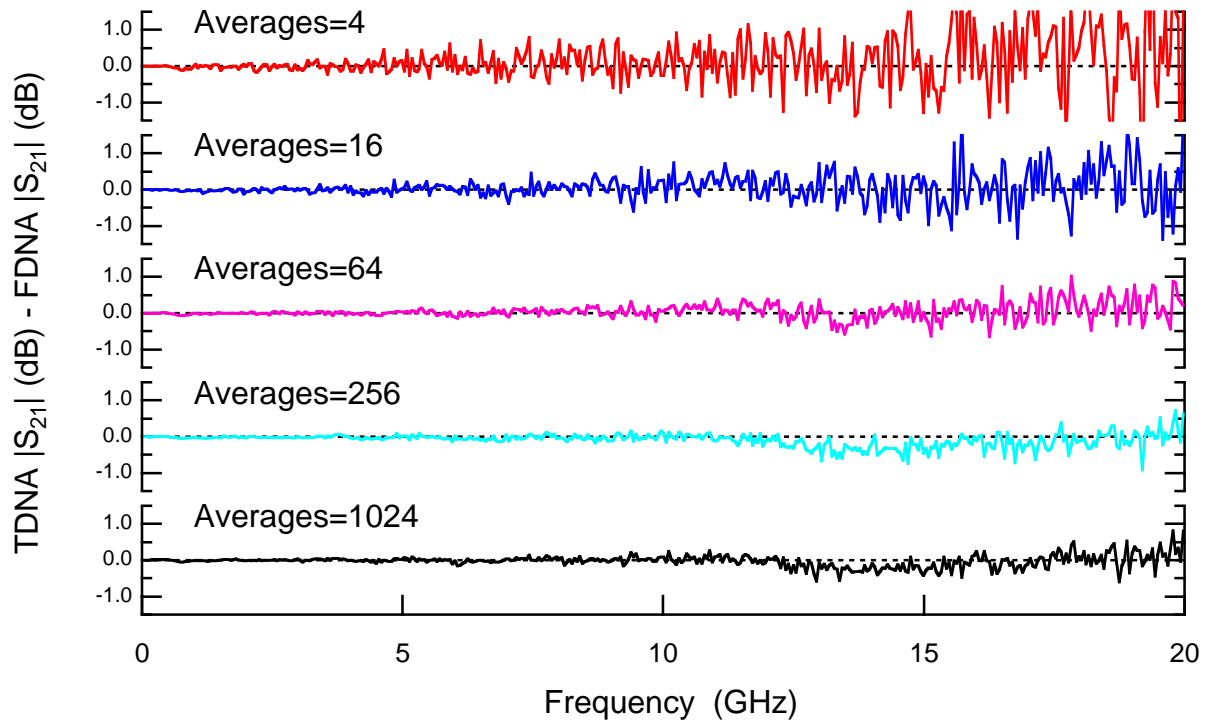TDNA Settings: 100 ns^{-1}, 256 avgs.

Fig. 11. Difference between TDNA and FDNA in S_{21} data from 20 mm line with differing averages. TDNA Settings = 100 ns^{-1}, 20.48 ns window. Only the number of averages changed.
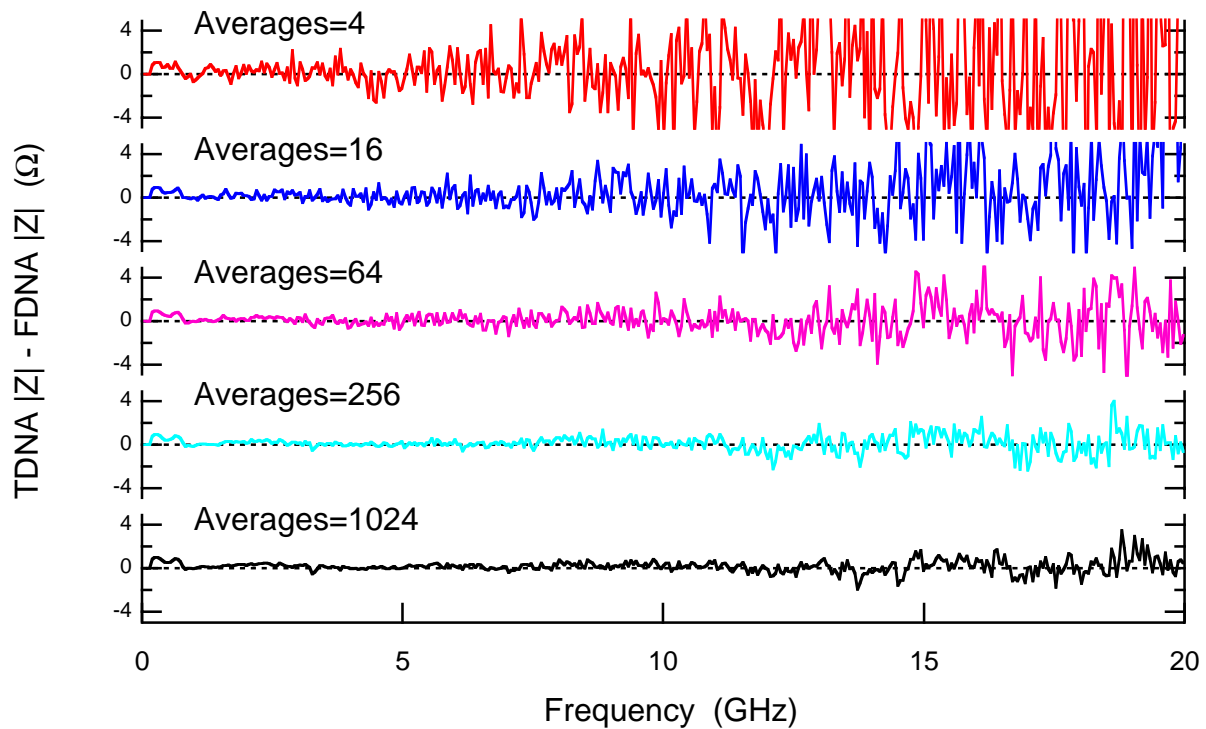

Fig. 11. Difference between TDNA and FDNA in Z data from CPW resistor with differing averages. TDNA Settings = 100 ns^{-1}, 20.48 ns window. Only the number of averages changed.